Current Pathobiology Reports (2019) 7:109–118
https://doi.org/10.1007/s40139-019-00203-8

UPDATE ON TECHNOLOGICAL INNOVATIONS FOR CANCER DETECTION AND TREATMENT (T DICKHERBER, SECTION EDITOR)

Highly Multiplexed, Quantitative Tissue Imaging at Cellular Resolution

Madeline E. McCarthy[1] · Marc R. Birtwistle[1]

Published online: 25 July 2019

Abstract

Purpose of Review There is a contemporary push to map tissues and their disease states quantitatively at single-cell and spatial resolution, but standard assays to do so, such as immunohistochemistry, have been historically lowly multiplexed (2–4 measurements). This push has driven the development of several new multiplexed techniques for quantitative tissue imaging, which we review here.

Recent Findings Standard multiplexed imaging is primarily limited by fluorophore spectral overlap. Innovations increasing multiplexing capacity include iterative cycles of staining/bleaching/imaging, imaging mass spectrometry with metal-conjugated antibodies, leveraging fluorophore combinatorics, and coupling to sequencing-based methods.

Summary Recent progress has increased image-based multiplexing roughly 10-fold and, in some cases of nucleic acid analytes, to genome scale. This has given unprecedented biological and disease knowledge, but there is still substantial work to achieve genome scale across all types of analytes, as well as spatial scales greater than ~millimeters. Concomitantly, challenges in data storage, retrieval, and analysis will need to be solved moving forward.

Keywords Imaging · Highly-multiplexed · Fluorescence · Mass spectrometry · Sequencing

Introduction

Human tissues consist of complex networks of interacting cells [1, 2, 3•, 4]. The architecture of a tissue, and to a large extent function, is defined by spatial organization of its cellular and extracellular compartments [5–7]. The architecture of normal and diseased tissues influences the development of a disease as well as receptiveness and resistance to therapy [8, 9]. The ability to characterize and gain further understanding of tissue architecture through imaging has driven progress in biology and pathology [10–13]. Immunohistochemistry (IHC) is a conventional tool used in clinical diagnostics and research laboratories to assess the spatial distribution of typically two to four analytes in a single sample [14–19]. However, IHC has a variety of limitations, such as the requirement of a new sample or serial section for each analyte set, which limits multiplexing, and non-linear relationships between analyte abundance and staining intensity (when fluorescence is not used), which limits quantification [20, 21]. Other methods exist which are highly multiplexed and provide quantitative data, such as deep sequencing, or even single-cell sequencing [22]. However, they have the limitation that spatial information in a tissue is often lost [23]. There is currently a large technological gap for methods that are image-based but offer more quantitative multiplexing at single-cell spatial resolution [20].

There are a variety of biological and disease applications for multiplexed tissue imaging; one example is cancer [20]. The NIH-funded Human Tumor Atlas Network was established to, in part, complement the tremendous efforts of The Cancer Genome Atlas with spatial information [24]. Tumor heterogeneity is multi-dimensional including variation in driver mutation profiles across space, extracellular matrix structure, soluble factor, and oxygen gradients, as well as multiple important cell types such as immune infiltrates and

This article is part of the Topical Collection on *Update on Technological Innovations for Cancer Detection and Treatment*

✉ Marc R. Birtwistle
mbirtwi@clemson.edu

[1] Department of Chemical and Biomolecular Engineering, Clemson University, Clemson, SC 29634, USA

tumor-associated fibroblasts that interact with tumor cells to influence tumor microenvironment [25•, 26–30]. This inherent tumor heterogeneity makes diagnosis, prognosis, and treatment a challenge because of its unknown impact on the tumor's evolution and drug sensitivity profile [25•, 31–33]. More highly multiplexed imaging tools and techniques will facilitate characterizing and better understanding tumor heterogeneity, helping to inform diagnosis, prognosis, and treatment.

In this review, we survey recent advances in image-based multiplexing technologies capable of single-cell spatial resolution, with focus as well on their quantitative features to some extent. Although major advances have been made with radiological methods including PET, CT, and MRI, we focus this review on techniques with higher spatial resolution and rather refer the reader to other resources on such topics [34–36]. These technologies can generally be divided into three categories: fluorescence-based, mass spectrometry-based, and very recently sequencing-based, which we enumerate below and are summarized in Table 1 and Fig. 1. These advances in imaging techniques have enabled the analysis of significantly more parameters in cells and tissues than what was previously possible, providing significant progress towards deeply characterizing the tumor microenvironment and other tissue or spatial analyses—a new grand challenge of biology for the twenty-first century post-genomic era.

Fluorescence-Based Methods

Central to fluorescence microscopy are fluorescent dyes attached to affinity binders, such as antibodies or oligonucleotides, which then associate with a targeted analyte, such as proteins, RNA, or DNA, allowing visualization and analysis [53]. Fluorescence-based methods can be divided into filter-based and spectral techniques. Filter-based fluorescence imaging uses optical films that allow relatively broad wavelength ranges of light to excite fluorophores in samples and the subsequent emission light to pass onto a detector, but multiplexing is limited usually to about four colors by inevitable spectral overlap. Spectral overlap occurs when fluorophore's excitation and/or emission spectra share substantial wavelength ranges, such that filters cannot efficiently separate them. Spectral (also called hyper-spectral) imaging partially overcomes this issue of overlap because much finer wavelength resolution for fluorescence emission is obtained [45, 54], by using, for example, monochromators, prisms, and/or diode arrays [55]. Currently, filter-based methods are the predominant modality because of simplicity and cost.

There are currently a wide variety of different fluorescent reporter agents available for these techniques. Examples include small organic molecules [56–58], fluorescent proteins [59–61], photo-switchable dyes [62–64], quantum dots [65–67], polymer dots [68, 69], and endogenous fluorescence [70–72]. The pros and cons of each of these are extensively discussed and reviewed as cited above, so we refer more interested readers there, but generally most fluorescent reporters are compatible across fluorescence-based imaging techniques.

Filter-Based

Filter-based fluorescence imaging is the most widely used method for visualizing cells and tissues. There are a variety of established textbook protocols (e.g., [73, 74]), and the required equipment is generally cheaper and more readily available than that for the methods that will be later described.

One way to achieve higher multiplexing is to simply perform repeated rounds of staining and imaging, with bleaching of fluorophores between rounds. Several recent techniques leverage this principle, including multiplexed fluorescence microscopy (MxIF) [37•], iterative indirect immunofluorescence imaging (4i) [38], cyclic immunofluorescence (CycIF) [39, 40••], and co-detection by indexing (CODEX) [41••]. These methods are in principle compatible with formalin-fixed paraffin-embedded (FFPE) tissue, a common format for preserving samples. They are limited by sample degradation across and the duration of each cycle.

MxIF measures up to 60 analytes in a single FFPE tissue section using fluorophore-conjugated primary antibodies [75]. The MxIF procedure consists of acquiring background autofluorescence, staining with four colors (one typically DAPI for nucleus fiduciary in each round), acquiring immunofluorescence, dye inactivation using alkaline oxidation chemistry, acquiring new background autofluorescence, restaining with new fluorescent dye-conjugated primary antibodies, and acquiring new images [37•]. The cycle is repeated until all target analytes are measured. This technique was used to examine colorectal cancer specimens and allowed the mapping of cellular mechanistic target of rapamycin complex 1 (mTORC1) and MAPK signal transduction patterns in tissues [37•], as well as in other applications [75, 76].

CycIF assembles up to 60-plex images of tissue sections via successive rounds of four-channel imaging [77], similarly to MxIF. Cycles involve four steps: immunostaining with fluorophore-conjugated primary antibodies, staining with a DNA dye to mark nuclei and facilitate image registration across cycles, four-channel imaging at low- and high magnification, and fluorophore bleaching (oxidation in a high pH hydrogen peroxide solution in the presence of light) followed by a wash step and then subsequent rounds of staining [39, 40••]. CycIF is partly limited not only by the assay duration as each cycle takes roughly 24 h to complete but also by sample degradation similar to MxIF [39, 77]. A major difference between CycIF and MxIF is that MxIF requires more expensive reagents and equipment, but has a shorter assay duration [78].

Table 1 Specifications of available highly multiplexed imaging methods. Important aspects of each method are described across columns.

		Principle of operation	Spatial resolution	Number of simultaneous measurements	Compatible assays	Assay duration
Fluorescence-based methods	Multiplexed fluorescence microscopy (MxIF)	Low-plex fluorescence images repeatedly collected using cycles of staining/bleaching/imaging	~200 nm	Up to 60 analyte/section	DNA FISH	2.5 h/cycle
	Iterative indirect immunofluorescence imaging (4i)	Low-plex fluorescence images repeatedly collected using cycles of staining/bleaching/imaging	~200 nm	~40 analytes/section	Not noted	Not reported
	Cyclic immunofluorescence (CycIF)	Low-plex fluorescence images repeatedly collected using cycles of staining/bleaching/imaging	~200 nm	~60 analytes/section	Super-resolution imaging, H&E	~24 h/cycle
	Co-detection by indexing (CODEX)	Uses DNA-conjugated antibodies as barcodes for fluorescence imaging multiplexing	~200 nm (fluorescence)	66/section	None noted	3.5 h/30 antibodies
	Super-resolution barcoding	Individual mRNAs are spatially resolved in diffraction-limited spots and identified with unique fluorophore barcodes	~5 nm	Up to ~30,000 mRNAs/section	Light sheet/selective plane illumination microscopy (SPIM)	Not reported
	Hyper-spectral fluorescence imaging	Measures fluorescence emission spectra in each pixel to allow linear unmixing of fluorophores with overlapping spectra	~200 nm	7 analyte/section	Fluorescence based modalities	Not Reported
	Multiplexing with spectral imaging and combinatorics (MuSIC)	Creates new independent probes from covalently linked combinations of individual fluorophores which are deconvolved through spectral imaging and linear unmixing	~200 nm	9 in restricted wavelength range, in principle ~30/section	Fluorescence based modalities	Not yet tested
	Spectrally resolved fluorescence lifetime imaging microscopy (sFLIM)	Combines spectral and fluorescence lifetime signatures to estimate fluorophore ratios in mixtures	~200 nm	9/section	None noted	Not reported
Mass spectrometry methods	Imaging mass cytometry	Metal-conjugated antibody levels are detected through mass spectrometry, and there is minimal overlap in mass-to-charge spectra between selected metals	~1000 nm	32/section	None noted	14 h/mm^2
	Multiplexed ion beam imaging (MIBI)	Metal-conjugated antibody levels are detected through mass spectrometry, and there is minimal overlap in mass-to-charge spectra between selected metals	~200 nm	40 experimentally demonstrated; ~7/cycle; up to 100 total	None noted	8 h per mm^2
Sequencing-based methods	Slide-seq	DNA-barcoded beads on a glass coverslip spatially capture mRNA from tissue	~10 μm	Transcriptome	None noted	~Days

	Quantitative?	Compatible with FFPE?	Major equipment	Major reagents	References
Fluorescence-based methods	Yes	Yes	Proprietary microscope	Fluorophore-conjugated primary antibodies; proprietary bleaches	Gerdes et al. [37•], McKinley et al. 2017
	Yes	No	Fluorescence microscope with the ability to remount samples multiple times (i.e., adequate *x-y* position recall)	Unconjugated primary and fluorophore-conjugated secondary antibodies	Gut et al. [38]
	Yes	Yes	Fluorescence microscope with the ability to remount samples multiple times (i.e., adequate *x-y* position recall)	Fluorophore-conjugated primary antibodies	Lin et al. [39], Lin et al. [40••]
	Yes	Yes	Fluorescence microscope	DNA-barcoded antibodies	Goltsev et al. [41••]
	Yes	No	Super-resolution microscope	Standard super-resolution imaging buffers; fluorophore-labeled oligo probes	Cai 2012, Lubeck and Cai [42], Cai, 2019
	Yes	Yes	Imaging spectrometer	Fluorophore-conjugated antibodies	Tsurui et al. [43•], Haraguchi et al. [44], Leavesley et al. 2011, Lu and Fei [45]
	Yes	Yes, in principle, but not yet evaluated	Imaging spectrometer	Fluorophore-conjugated primary antibodies	Holzapfel et al. [46••]
	Yes	Not reported	Microscope with time-resolved fluorescence lifetime and spectral imaging capabilities	Fluorophore-conjugated antibodies	(Niehörster et al. [47])
Mass spectrometry methods	Yes	Yes	Inductively coupled plasma mass spectrometry instrument and laser ablation system	Metal-conjugated antibodies	Giesen et al. [48•], Chang et al. 2017, Bodenmiller 2016
	Yes	Yes	Mass spectrometer and an O- primary ion beam for ablation	Metal-conjugated antibodies	Angelo et al. [49], Bodenmiller [50]
Sequencing-based methods	Yes	Not reported	SOLiD sequencing (and Illumina but that is more standard)	SOLiD reagents/beads for mRNA capture	Rodriques et al. [51••]

TOF time of flight

FISH fluorescence in situ hybridization

H&E hemotoxylin and eosin

The 4i method can detect up to 40 analytes [38]. So-called "indirect immunofluorescence" uses an unconjugated primary antibody and a fluorophore-conjugated secondary antibody, rather than a single primary antibody directly conjugated to the fluorophore, resulting in compatibility with "off-the-shelf" antibodies. This is the main distinctive feature of 4i. The 4i technique has been used to create multiplexed protein maps in different phases of the cell cycle, in response to cell crowding, inhibitors, and different growth conditions [79].

CODEX has visualized up to 66 DNA-conjugated antibodies in a single image [41••]. The barcode information is encoded by an overhang sequence on the DNA duplex that is read off in cycles of two-color imaging. Thus, 66 antibodies need 33 rounds of imaging. Overhang lengths on each antibody can be as small as two (1 color code) or as large as feasible for the experiment time scale and sample degradation of cycling. Two types of "walking" nucleotides (G and A) are used to traverse the overhang, and then, other two (U and T) are labeled with either Cy3 or Cy5, respectively. First, a reaction mixture leaving out A is incubated on the antibody-stained sample. Only overhangs with C as the first base in its sequence are capable of incorporating a fluorescently labeled nucleotide, and then, CG would get a Cy3 label, and CA would get a Cy5 label. Other overhangs with a CT sequence do not yet receive a color. Next, a reaction mixture leaving out G is incubated on the sample. Then, CTG would get a Cy3 label, and CTA would get a Cy5 label. Other overhangs with a CTC sequence do not yet receive a color. This strategy is repeated for multiple rounds of extension on the overhang to perform the multiplexed imaging. Thus, the barcode is then the combination of the round in which a signal was detected, plus whether the color was Cy3 or Cy5. CODEX was used to determine that significant changes in expression levels in certain markers, such as B220, CD79b, or CD27, are dependent on the tissue microenvironment in which the cells reside [41••]. This drove the conclusion that cell populations that are currently thought of as broadly expressing a certain marker are actually comprised of multiple subphenotypes that correlate with the indexed niche identity [41••].

There are also non-spectral techniques that do not involve cycles of imaging, but rather use super-resolution microscopy and combinatorial labeling [42]. This method has many similarities to standard fluorescence in situ hybridization (FISH) involving fluorophore-conjugated oligonucleotide probes complementary to mRNA targets [80–82]. However, because in super-resolution microscopy, which drives beyond the diffraction limit, each mRNA molecule can be spatially resolved in a single pixel (or voxel) and can hybridize to several different color probes, the potential combination of fluorophores in each pixel (or voxel) can be used to multiplex mRNA measurements. Simple counting of spots with matched fluorophore combination barcodes is the quantitative readout. In proof-of-principle studies, three color barcodes with seven fluorophores were used to profile transcripts from 32 stress-responsive genes in single *Saccharomyces cerevisiae* cells. Thus, a transcript is defined by a combination of 3 colors from 7 choices. The results were confirmed to match to those expected from more conventional readouts [42, 83].

In a recent follow-up, this approach was scaled transcriptome wide (~30,000 transcripts/cell), in a technique called seqFISH+, which combines the super-resolution notion with the repeated rounds of imaging principal from above [84••]. Here, the innovation was switching from transcripts having real color barcodes to having "pseudo-color" barcodes. Now, each transcript is only labeled with a single color fluorophore, but is assigned a pseudo-color (1 to 20) based on when this fluorescence signal is observed over 20 sequential rounds of hybridization. This has the added benefit of having only 1/20th of the transcripts in the cell showing a signal in a particular image. Then, these 20 sequential rounds of imaging are repeated 4 separate times in an "outer loop" of barcoding rounds. In barcoding rounds, the hybridization round where a fluorescence signal appears (1 to 20) can be different for each gene, giving rise to a possible number of permutations on par with the genome.

Another non-spectral technique that does not involve cycles of imaging is fluorescence lifetime imaging microscopy (FLIM). FLIM works by determining the lifetime of the excited state in order to characterize the molecular species [85]. Within FLIM, there are two distinct methods; the time-domain method and frequency-domain method [86, 87]. Time-domain FLIM works by collecting the temporal emission profile at each pixel. This is then fit to an exponential curve to determine the fluorescence lifetime [87, 88]. Frequency-domain FLIM operates by varying excitation intensity sinusoidally over time and then determining the phase and amplitude shifts of the emission as a function of the sinusoidal frequency. These shifts are related to the fluorescence lifetime [89]. These two complementary methods have their own advantages and disadvantages. Time-domain FLIM has a higher sensitivity for measurements with low fluorescence with a single-photon timing technique, whereas frequency-domain FLIM is generally faster and electronics are simpler [86, 89]. The basis by which fluorescence lifetime can increase multiplexing is by finding fluorophore combinations that can be separated by short vs. long lifetimes, although this is not a common approach.

Sample quality becomes increasingly important with cycles of imaging and can become a major limiting factor for these methods. For CyCIF, it was found that half of the tissue samples tested could be routinely imaged up to 15 cycles with 20% loss of cells [40••]. However, it should be noted that sample degradation widely varied across tissue types (Fig. 4E from [40••]). Thus, extensive work remains to better characterize how different tissue/cell type samples and also how their mode of preparation (FFPE/frozen/etc.) impacts

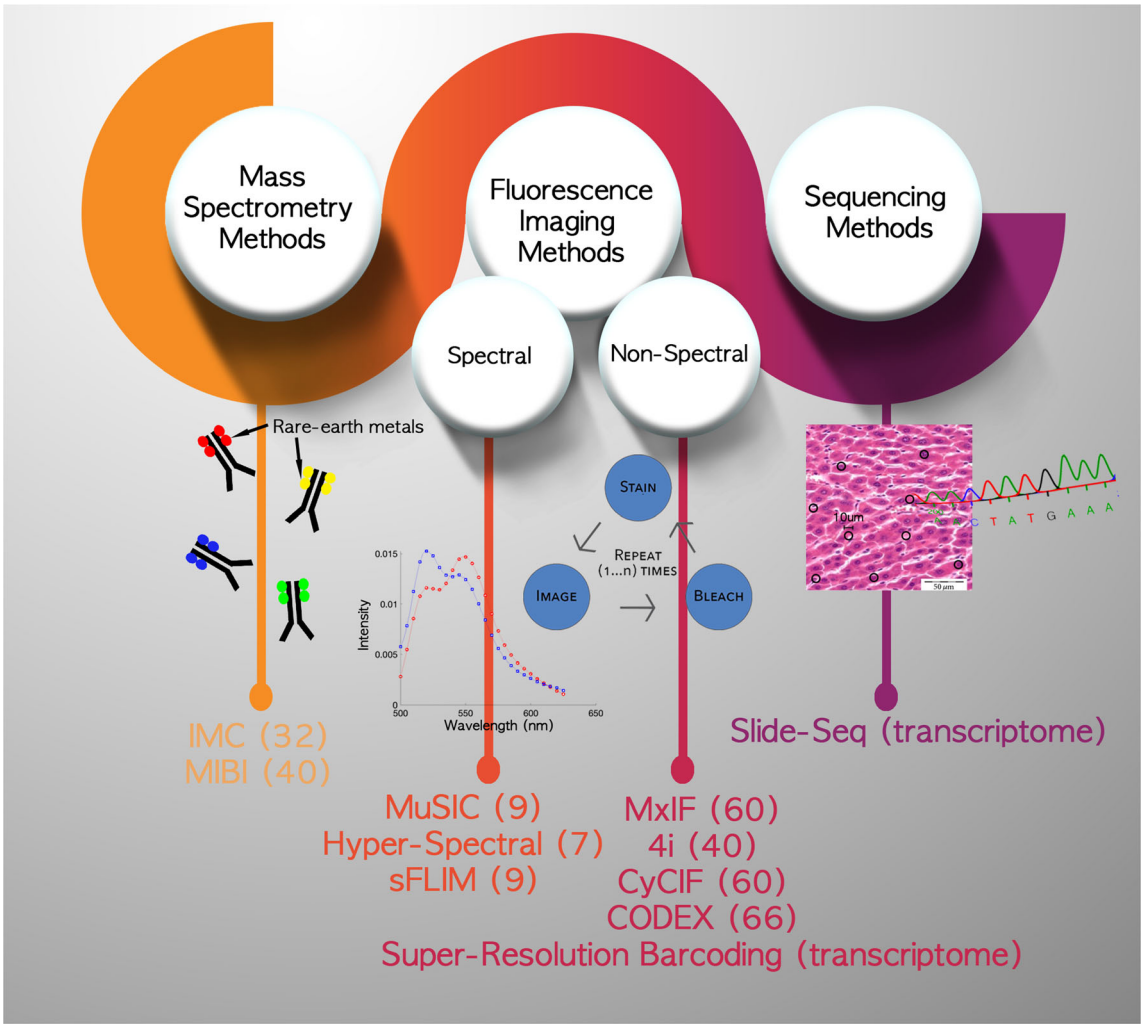

Figure 1 Schematic of available highly multiplexed imaging methods. The current highly multiplexed imaging techniques can be grouped into three general categories: mass spectrometry-based, fluorescence-based, and sequencing-based. Technique names are indicated with their reported multiplexing capacity in parentheses. Rare earth metals attached to antibodies are depicted for mass spectrometry. The fluorescence imaging methods can be further divided into spectral and non-spectral subcategories. Fluorescence emission spectral scan data for two fluorophores exhibiting ± FRET is shown. The general cycling procedure for multiplexing is depicted for non-spectral fluorescence imaging. Sequencing data can be obtained from 10-μm diameter sections in tissue samples. Tissue image from Al-Rasheed et al. [52]

the ability to apply multiplexing methods by repeated round of imaging.

Spectral

Spectral imaging acquires much finer emission wavelength information than non-spectral imaging, which allows one to quantify mixtures of fluorophores with potentially heavily overlapping spectra. Similar to filter-based techniques, spectral imaging might also be performed using multiple rounds of labeling, although this has not yet been described to our knowledge. However, it is currently less popular than non-spectral imaging because the equipment is more expensive, and the technique is less established and therefore more difficult.

Spectral imaging techniques are largely called hyperspectral and have been used to image up to seven analytes simultaneously in tissues [43•, 44, 45, 90, 91], and even live cells [92]. Analysis is broadly called linear unmixing, which applies the principle of additivity of fluorescence emission spectra to cast a linear algebra problem, which when solved gives the levels of the individual fluorophores in each pixel. Multiple fluorophores from ultraviolet to infrared are used with (typically) three (or more) excitation channels. Design of spectral imaging experiments is more complex than filter-based, but there are metrics that can be used to help, such as the figure of merit (FoM) [93•]. The FoM indicates how well a given imaging protocol performs for a set of fluorophores, relative to the case that these fluorophores are present singularly and that their fluorescence can be measured noiselessly

[93•]. Many modern and widely available confocal microscopes also have an ability to perform emission spectral scans. Hyper-spectral fluorescence imaging has a variety of medical applications, including disease diagnosis and image-guided surgery [45]. Although not tissue imaging, also of note are recent flow cytometers that can perform spectral imaging, such as Cytek Aurora [94].

Fluorescence multiplexing using spectral imaging and combinatorics (MuSIC) builds on spectral imaging but uses single or covalent combinations of existing fluorophores to significantly increase the number of multiplexed analytes [46••]. If a fluorophore covalent combination probe exhibits significant Förster resonance energy transfer (FRET), then mathematically, adding this probe to the linear unmixing problem is "well-posed," and its levels can be estimated along with the single fluorophores that make up the combination. Multiplexing up to 9 such MuSIC probes was demonstrated in solution-based assays over a restricted excitation wavelength window (~ 1/4 of that available), and it has the potential to scale to ~ 30 analytes [46••]. MuSIC is compatible with the bleach-and-restain ideas from above, so multiplexing is potentially multiplicative when combining the two ideas. Moreover, because it has been shown to be compatible with fluorescent proteins, it is in principle compatible live cells or tissues.

Another method for spectral imaging is spectrally resolved fluorescence lifetime imaging microscopy (sFLIM). sFLIM combines multiple excitation wavelengths (485 nm, 532 nm, and 640 nm), time-domain FLIM via time-correlated single-photon counting (TCSPC), and a diode array for 32 spectrally separated detection channels [47]. A "pattern-matching" algorithm (similar to linear unmixing) is used to determine the individual contribution from each fluorophore to the overall multi-dimensional (spectra + lifetime) fluorescence signal. The algorithm is based on reference patterns of fluorescence decay and spectral signatures from various cell samples that are labeled with different fluorescent probes. sFLIM has been used to visualize nine different target molecules simultaneously in mouse C2C12 cells [47].

Mass Spectrometry-Based Methods

In addition to fluorescence, there are also highly multiplexed mass spectrometry methods for tissue imaging. Here, cells are typically stained with metal-conjugated antibodies, whose levels then can be quantified with mass spectrometry [49]. It is easier to multiplex using mass spectrometry as compared with fluorescence imaging because there is negligible spectral overlap. Signal-to-noise is also improved because employed metals are essentially non-existent in tissues. However, the specialized mass spectrometry equipment (and to some extent reagents) that interfaces with imaging is significantly more expensive and not as widely available.

Current mass spectrometry methods include imaging mass cytometry (IMC) [48•] and multiplexed ion beam imaging (MIBI) [49], both of which multiplex using a panel of primary antibodies conjugated with isotopically pure, rare-earth elements (e.g., lanthanides) [48•]. Metals are conjugated to antibodies via a polymeric metal-chelating linker that is covalently linked to antibodies, or with metal nanoparticles [95]. In IMC, once a tissue sample has been stained with the metal-conjugated antibodies, it is dried and then positioned in a laser ablation chamber [48•]. The tissue is then ablated spot by spot and line by line, which sends material via a mixed argon and helium stream to a CyTOF mass cytometer [48•]. This method is capable of 32 simultaneous measurements [50]. IMC has been used to assess the immune microenvironment in breast cancer tissue, leading to the hypothesis that trastuzumab-treated patients with high tumor-infiltrating lymphocyte levels have improved outcomes [96]. MIBI is similar to IMC, but uses an ion beam ablation (rather than a laser), and thus has slightly different mass spectrometry requirements [48•, 49, 50, 95]. Biological specimens are immobilized on a conductive substrate, stained with metal-conjugated antibodies, dried, and loaded under vacuum for MIBI analysis [49]. This method has been used to image 40 analytes simultaneously in breast tumor tissue sections, but is potentially capable of up to 100 [49, 97].

Sequencing-Based Methods

So far, highly multiplexed sequencing methods that have transformed genomics, transcriptomics, and epigenomics have not been highly compatible with imaging. However, a recent technological advancement called Slide-seq has enabled the transfer of RNA from tissue sections onto a surface packed with DNA-barcoded beads at specified positions, allowing the spatial analysis of gene expression in a tissue at ~ 10-μm resolution [51••]. This method first involves packing of the DNA-barcoded beads on to a rubber-coated glass coverslip, called the "puck." This is followed by oligonucleotide ligation and detection (SOLiD) sequencing to determine each bead's distinct sequence and *x-y* location [51••]. A tissue section is placed on the "puck," and mRNA from the tissue is captured by the beads with minimal lateral *x-y* diffusion. After capture, the bead/tissue section combination is homogenized and prepared for mRNA sequencing (via more standard Illumina-based methods), which subsequently allows relating transcriptomes to spatial locations. Using Slide-seq, it was determined that cell proliferation occurs in the first few days after a traumatic brain injury and then transitions to differentiation in the following weeks [51••]. The main costs associated with this method seem to be related to the price of the pucks. As the price of these "pucks" and the associated sequencing drop, there is potential to be able to apply this method to entire organs or even entire organisms [51••]. One could

similarly envision coupling other nucleic acid-based conjugate technologies to enable Slide-seq on analytes other than mRNAs.

Data Analysis

Multiplexed image data are powerful but also come with several data handling, visualization, and analysis challenges, which are just beginning to be explored. Some of these techniques include viSNE, which is used for dimensionality reduction [98], multi-omics heterogeneity analysis (MOHA), which is used for image processing and visualization [25•], open microscopy environment remote objects (OMERO) servers, which are used for data handling, and multiplex image cytometry analysis (miCAT/histoCAT), which is for data handling and analysis [99, 100]. viSNE is a technique that allows visualization of high-dimensional single-cell data on a two-dimensional map and is based on the now widespread t-distributed stochastic neighbor embedding (t-SNE) algorithm [98, 101]. In this method, each cell is represented as a point in high-dimensional analyte space, with each dimension being measurement of one analyte [98]. An optimization algorithm searches for a projection of the points from the high-dimensional space into two or three dimensions to the extent that pairwise distances (e.g., Euclidian) between two points (cells) are best conserved between the high- and low-dimensional space [98]. Coupled with mass cytometry, viSNE was used to compare leukemia diagnosis and relapse samples [98]. This method could also be applied to IMC or MIBI but requires additional image analysis steps to obtain single-cell data.

The MOHA tool computes tissue heterogeneity metrics from multiplexed image data by combining single-cell molecular summary measures with pre-existing knowledge of biological pathways to assign states to cells in the tissue [25•]. This is followed by using positional cell information to compute spatial cell state distributions, and importantly, correlations between neighboring cell types. It then computes tissue heterogeneity and diversity measures of the cells from the observed distributions of these molecular and spatially defined states [25•]. This technique was used to identify statistically significant correlations between the intratumoral AKT pathway state diversity and cancer stage and histological tumor grade [25•].

OMERO is a flexible software platform that provides a structured storage format for a range of biological data, including images [102]. It is used to provide storage access, processing, and visualization without downloading entire datasets [102]. OMERO has been used in a variety of applications, including CycIF [40••].

miCAT and histoCAT are analysis platforms that are used for quantitative and comprehensive visualization of cell phenotypes, cell interactions, microenvironments, and tissue structures [99, 100]. They are coupled with IMC to investigate cellular phenotypes and microenvironments of human breast cancer, allowing insight into the network structure of cell neighborhood interactions [99, 100].

Conclusion

The methods described here have increased our ability to quantitatively understand the interactions between different biological components in tissues and the regulatory networks in single cells, but importantly, retaining information on how it was arranged spatially. This has and will continue to transform our ability to understand biology and disease. Although multiplexed tissue imaging has come a long way in the past decade, there remains much work to be done to go from the currently possible dozens of measurements to the proteome scale, especially with post-translational modifications. Very recent methods have begun to approach this scale for the transcriptome. The possibility of combining methods described here could multiplicatively increase the amount of quantitative information that can be obtained. For example, CycIF might be combined with super-resolution imaging, and/or with MuSIC-based approaches to increase the potential number of simultaneous measurements. Moreover, it is not only multiplexing that needs to improve further. Currently, covering more than ~millimeter length scales comprehensively is extremely challenging other than by brute force with time and money; innovation here is also needed to truly multiplex tissue imaging, where important changes happen over centimeter (and greater) scales. Tissue clearing techniques will likely play a large role here [3•]. As these types of data become increasingly available, storing the very large raw amounts of data, in addition to analyzing them, will present major bottlenecks. We expect yet still much innovation in these directions in the next several years towards the genome scale, whole-tissue, or even whole-body quantitative, single-cell imaging end goal.

Acknowledgments We thank Stephanie Klaubert for the discussions and Chloe Worthy and Althea Henderson for the help with illustration.

Funding Information MRB received funding from Clemson University and the NIH Grant R21CA196418.

Compliance with Ethical Standards

Conflict of Interest Madeline E. McCarthy and Marc R. Birtwistle each declare no potential conflicts of interest.

Human and Animal Rights and Informed Consent This article does not contain any studies with human or animal subjects performed by any of the authors.

References

Papers of particular interest, published recently, have been highlighted as:
- • Of importance
- •• Of major importance

1. Koifman G, Aloni-Grinstein R, Rotter V. p53 balances between tissue hierarchy and anarchy. J Mol Cell Biol. 2019.
2. Griffith LG, Swartz MA. Capturing complex 3D tissue physiology in vitro. Nat Rev Mol Cell Biol. Mar. 2006;7:211–24.
3.• Tainaka K, et al. Whole-body imaging with single-cell resolution by tissue decolorization. *Cell*. 2014;159(4):911–24 **This study gives an efficient whole-organ and whole-body clearing protocol.**
4. Gerner MY, Kastenmuller W, Ifrim I, Kabat J, Germain RN. Histo-cytometry: a method for highly multiplex quantitative tissue imaging analysis applied to dendritic cell subset microanatomy in lymph nodes. Immunity. 2012;37(2):364–76.
5. Bissell MJ, Rizki A, Mian IS. Tissue architecture: the ultimate regulator of breast epithelial function. Curr Opin Cell Biol. 2003;15(6):753–62.
6. Sasai Y. Cytosystems dynamics in self-organization of tissue architecture. Nature. 2013;493(7432):318–26.
7. Wedeen VJ, Hagmann P, Tseng W-YI, Reese TG, Weisskoff RM. Mapping complex tissue architecture with diffusion spectrum magnetic resonance imaging. Magn Reson Med. 2005;54(6): 1377–86.
8. Cohen AS, Morse DL, Chen T, Rejniak KA, Estrella V, Lloyd MC. The role of tumor tissue architecture in treatment penetration and efficacy: an integrative study. *Front Oncol*. 2013;3(May):1–13.
9. Nelson CM, Bissell MJ. Of extracellular matrix, scaffolds, and signaling: tissue architecture regulates development, homeostasis, and cancer. Annu Rev Cell Dev Biol. Oct. 2006;22(1):287–309.
10. Kherlopian AR, et al. A review of imaging techniques for systems biology. BMC Syst Biol. 2008;2:1–18.
11. Micheva KD, Smith SJ. Array tomography: a new tool for imaging the molecular architecture and ultrastructure of neural circuits. Neuron. 2007;55(1):25–36.
12. Hama H, Kurokawa H, Kawano H, Ando R, Shimogori T, Noda H, et al. Scale: a chemical approach for fluorescence imaging and reconstruction of transparent mouse brain. Nat Neurosci. Aug. 2011;14:1481–8.
13. Lee E, Choi J, Jo Y, Kim JY, Jang YJ, Lee HM, et al. ACT-PRESTO: rapid and consistent tissue clearing and labeling method for 3-dimensional (3D) imaging. Sci Rep. Jan. 2016;6:18631.
14. Roelofs AJ, De Bari C. Immunostaining of skeletal tissues. In: *Methods in molecular biology*, vol. 1914; 2019. p. 437–50.
15. Intartaglia M, Sabetta R, Gargiulo M, Roncador G, Marino FZ, Franco R. Immunohistochemistry for cancer stem cells detection: principles and methods. In: Papaccio G, Desiderio V, editors. Cancer stem cells: methods and protocols. New York, NY: Springer New York; 2018. p. 195–211.
16. Ouyang N, Wang L. Basic histopathological methods and breast lesion types for research. In: Cao J, editor. Breast cancer: methods and protocols. New York, NY: Springer New York; 2016. p. 3–9.
17. Taylor CR. Immunohistochemistry in surgical pathology: principles and practice. In: Day CE, editor. Histopathology: methods and protocols. New York: Springer New York; 2014. p. 81–109.
18. Sedgewick J. Imaging techniques in signal transduction IHC. In: Kalyuzhny AE, editor. Signal transduction immunohistochemistry: methods and protocols. Totowa: Humana Press; 2011. p. 113–42.
19. Robertson D, Savage K, Reis-Filho JS, Isacke CM. Multiple immunofluorescence labelling of formalin-fixed paraffin-embedded (FFPE) tissue. BMC Cell Biol. 2008;9:1–10.
20. Rimm DL. What brown cannot do for you. Nat Biotechnol. 2006;24(8):914–6.
21. Jensen K, Krusenstjerna-Hafstrøm R, Lohse J, Petersen KH, Derand H. A novel quantitative immunohistochemistry method for precise protein measurements directly in formalin-fixed, paraffin-embedded specimens: analytical performance measuring HER2. Mod Pathol. Oct. 2016;30:180.
22. Islam S, Kjällquist U, Moliner A, Zajac P, Fan JB, Lönnerberg P, et al. Highly multiplexed and strand-specific single-cell RNA 5′ end sequencing. Nat Protoc. Apr. 2012;7:813–28.
23. Ren X, Kang B, Zhang Z. Understanding tumor ecosystems by single-cell sequencing: promises and limitations. *Genome Biol*. 2018;19(1):211.
24. NIH. Department of Health and Human Services part 1 . Overview information. *Natl Inst Heal RFA-AI-14-047*. 2014;10:1–3.
25.• Graf JF, Zavodszky MI. Characterizing the heterogeneity of tumor tissues from spatially resolved molecular measures. *PLoS One*. 2017;12(11):1–20 **The study describes a tool to compute tissue heterogeneity metrics from MxIF spatially resolved tissue imaging data.**
26. Alizadeh AA, Aranda V, Bardelli A, Blanpain C, Bock C, Borowski C, et al. Toward understanding and exploiting tumor heterogeneity. Nat Med. Aug. 2015;21:846–53.
27. O'Connor JPB, Rose CJ, Waterton JC, Carano RAD, Parker GJM, Jackson A. Imaging intratumor heterogeneity: role in therapy response, resistance, and clinical outcome. Clin Cancer Res. 2015;21(2):249–57.
28. Sottoriva A, Spiteri I, Piccirillo SGM, Touloumis A, Collins VP, Marioni JC, et al. Intratumor heterogeneity in human glioblastoma reflects cancer evolutionary dynamics. Proc Natl Acad Sci U S A. Mar. 2013;110(10):4009–14.
29. Gerlinger M, Rowan AJ, Horswell S, Math M, Larkin J, Endesfelder D, et al. Intratumor heterogeneity and branched evolution revealed by multiregion sequencing. N Engl J Med. Mar. 2012;366(10):883–92.
30. Landau DA, Carter SL, Stojanov P, McKenna A, Stevenson K, Lawrence MS, et al. Evolution and impact of subclonal mutations in chronic lymphocytic leukemia. Cell. 2013;152(4):714–26.
31. Gerdes MJ, et al. Single-cell heterogeneity in ductal carcinoma in situ of breast. Mod Pathol. 2018;31(3):406–17.
32. Marusyk A, Polyak K. Tumor heterogeneity: causes and consequences. Biochim Biophys Acta. Jan. 2010;1805(1):105–17.
33. Tsujikawa T, Kumar S, Borkar RN, Azimi V, Thibault G, Chang YH, et al. Quantitative multiplex immunohistochemistry reveals myeloid-inflamed tumor-immune complexity associated with poor prognosis. Cell Rep. 2017;19(1):203–17.
34. Kobayashi H, Longmire MR, Ogawa M, Choyke PL, Kawamoto S. Multiplexed imaging in cancer diagnosis: applications and future advances. Lancet Oncol. Jun. 2010;11(6):589–95.
35. Lee H, Langham MC, Rodriguez-Soto AE, Wehrli FW. Multiplexed MRI methods for rapid estimation of global cerebral metabolic rate of oxygen consumption. Neuroimage. Apr. 2017;149:393–403.
36. Yang M, Gao H, Sun X, Yan Y, Quan Q, Zhang W, et al. Multiplexed PET probes for imaging breast cancer early response to $VEGF_{121}$/rGel treatment. Mol Pharm. Apr. 2011;8(2):621–8.
37.• Gerdes MJ, et al. Highly multiplexed single-cell analysis of formalin-fixed, paraffin-embedded cancer tissue. *Proc Natl Acad Sci*.

2013;110(29):11982–7 **This study provided the first technique for cyclic fluorescence tissue imaging.**

38. Gut G, Herrmann MD, Pelkmans L. Multiplexed protein maps link subcellular organization to cellular states. Science. 2018;361(6401):eaar7042.
39. Lin JR, Fallahi-Sichani M, Chen JY, Sorger PK. Cyclic immunofluorescence (CycIF), a highly multiplexed method for single-cell imaging. Curr Protoc Chem Biol. 2016;8(4):251–64.
40.•• Lin JR, et al. Highly multiplexed immunofluorescence imaging of human tissues and tumors using t-CyCIF and conventional optical microscopes. *Elife*. 2018;7:1–46 **This technique provided a cost-effective method for cyclic fluorescence imaging.**
41.•• Goltsev Y, et al. Deep profiling of mouse splenic architecture with CODEX multiplexed imaging. *Cell*. 2018;174(4):968–981.e15 **This method visualizes up to 66 antibodies using barcodes and cycles of imaging.**
42. Lubeck E, Cai L. Single-cell systems biology by super-resolution imaging and combinatorial labeling. Nat Methods. 2012;9(7):743–8.
43.• Tsurui H, Nishimura H, Hattori S, Hirose S, Okumura K, Shirai T. Seven-color fluorescence imaging of tissue samples based on fourier spectroscopy and singular value decomposition. *J Histochem Cytochem*. 2000;48(5):653–62 **This study is one of the first techniques for spectral fluorescence imaging.**
44. Haraguchi T, Shimi T, Koujin T, Hashiguchi N, Hiraoka Y. Spectral imaging fluorescence microscopy. Genes Cells. 2002;7(9):881–7.
45. Lu G, Fei B. Medical hyperspectral imaging: a review. *J Biomed Opt*. 2014;19(1):010901.
46.•• Holzapfel HY, et al. Fluorescence multiplexing with spectral imaging and combinatorics. *ACS Comb Sci*. 2018;20(11):653–9 **This paper significantly scales up the number of analytes that can be measured using spectral imaging.**
47. Niehörster T, Löschberger A, Gregor I, Krämer B, Rahn HJ, Patting M, et al. Multi-target spectrally resolved fluorescence lifetime imaging microscopy. Nat Methods. Jan. 2016;13:257–62.
48.• Giesen C, et al. Highly multiplexed imaging of tumor tissues with subcellular resolution by mass cytometry. *Nat Methods*. 2014;11(4):417–22 **This technique uses metal-conjugated antibodies and mass cytometry to produce highly multiplexed images.**
49. Angelo M, Bendall SC, Finck R, Hale MB, Hitzman C, Borowsky AD, et al. Multiplexed ion beam imaging (MIBI) of human breast tumors. Nat Med. 2014;20(4):436–42.
50. Bodenmiller B. Multiplexed epitope-based tissue imaging for discovery and healthcare applications. Cell Syst. 2016;2(4):225–38.
51.•• Rodriques SG, et al. Slide-seq: a scalable technology for measuring genome-wide expression at high spatial resolution. *Science (80-)*. 2019;363(6434):1463–7 **This study provides a technique for spatially resolved high throughput sequencing of mRNAs.**
52. Al-Rasheed NM, Attia HA, Mohamad RA, Al-Rasheed NM, Al-Amin MA, AL-Onazi A. Aqueous Date Flesh or Pits Extract Attenuates Liver Fibrosis via Suppression of Hepatic Stellate Cell Activation and Reduction of Inflammatory Cytokines, Transforming Growth Factor- β 1 and Angiogenic Markers in Carbon Tetrachloride-Intoxicated Rats. Evidence-Based Complement. Altern Med. 2015;2015:1–19.
53. Dobrucki JW, Kubitscheck U. Fluorescence microscopy. In: Fluoresc Microsc From Princ to Biol Appl, vol. 2, no. 12. Second ed; 2017. p. 85–132.
54. Gao L, Hagen N, Tkaczyk TS. Quantitative comparison between full-spectrum and filter-based imaging in hyperspectral fluorescence microscopy. J Microsc. 2012;246(2):113–23.
55. Leavesley SJ, Annamdevula N, Boni J, Stocker S, Grant K, Troyanovsky B, et al. Hyperspectral imaging microscopy for identification and quantitative analysis of fluorescently-labeled cells in highly autofluorescent tissue. J Biophotonics. 2012;5(1):67–84.
56. Terai T, Nagano T. Small-molecule fluorophores and fluorescent probes for bioimaging. Pflugers Arch - Eur J Physiol. 2013;465(3):347–59.
57. Wysocki LM, Lavis LD. Advances in the chemistry of small molecule fluorescent probes. Curr Opin Chem Biol. Dec. 2011;15(6):752–9.
58. Luo S, Tan X, Fang S, Wang Y, Liu T, Wang X, et al. Mitochondria-targeted small-molecule fluorophores for dual modal cancer phototherapy. Adv Funct Mater. May 2016;26(17):2826–35.
59. Chudakov DM, Matz MV, Lukyanov S, Lukyanov KA. Fluorescent proteins and their applications in imaging living cells and tissues. Physiol Rev. Jul. 2010;90(3):1103–63.
60. Shaner NC, Steinbach PA, Tsien RY. A guide to choosing fluorescent proteins. Nat Methods. 2005;2(12):905–9.
61. Hoffman RM. The multiple uses of fluorescent proteins to visualize cancer in vivo. Nat Rev Cancer. 2005;5(10):796–806.
62. Bates M, Huang B, Dempsey GT, Zhuang X. Multicolor super-resolution imaging with photo-switchable fluorescent probes. Science(80-). 2007;317(5845):1749 LP–1753.
63. Habuchi S, Tsutsui H, Kochaniak AB, Miyawaki A, van Oijen AM. mKikGR, a monomeric photoswitchable fluorescent protein. *PLoS One*. 2008;3(12):e3944.
64. Bates M, Huang B, Zhuang X. Super-resolution microscopy by nanoscale localization of photo-switchable fluorescent probes. Curr Opin Chem Biol. Oct. 2008;12(5):505–14.
65. Ma Q, Su X. Recent advances and applications in QDs-based sensors. Analyst. 2011;136(23):4883–93.
66. Michalet X, et al. Quantum dots for live cells, in vivo imaging, and diagnostics. *Science (80-)*. 2005;307(5709):538 LP–544.
67. Medintz IL, Uyeda HT, Goldman ER, Mattoussi H. Quantum dot bioconjugates for imaging, labelling and sensing. Nat Mater. 2005;4(6):435–46.
68. Wu C, Chiu DT. Highly fluorescent semiconducting polymer dots for biology and medicine. Angew Chem Int Ed. 2013;52(11):3086–109.
69. Liu H-Y, Wu PJ, Kuo SY, Chen CP, Chang EH, Wu CY, et al. Quinoxaline-based polymer dots with ultrabright red to near-infrared fluorescence for in vivo biological imaging. J Am Chem Soc. Aug. 2015;137(32):10420–9.
70. Brancaleon L, Durkin AJ, Tu JH, Menaker G, Fallon JD, Kollias N. In vivo fluorescence spectroscopy of nonmelanoma skin cancer¶. Photochem Photobiol. Feb. 2001;73(2):178–83.
71. Reinert KC, Dunbar RL, Gao W, Chen G, Ebner TJ. Flavoprotein autofluorescence imaging of neuronal activation in the cerebellar cortex in vivo. J Neurophysiol. Jul. 2004;92(1):199–211.
72. Brookner CK, Follen M, Boiko I, Galvan J, Thomsen S, Malpica A, et al. Autofluorescence patterns in short-term cultures of normal cervical tissue. Photochem Photobiol. Jun. 2000;71(6):730–6.
73. Paddock SW, Confocal Microscopy, vol. 122 1st ed. New Jersey: Humana Press; 1998.
74. Verveer PJ, editor. Advanced fluorescence microscopy, vol. 1251. New York: Springer New York; 2015.
75. cKinley ET et al. Optimized multiplex immunofluorescence single-cell analysis reveals tuft cell heterogeneity. JCI Insight. 2017;2(11).

76. Nadarajan G, et al. Automated multi-class ground-truth labeling of H&E images for deep learning using multiplexed fluorescence microscopy. In: *Proc.SPIE*, vol. 10956; 2019.
77. Lin JR, Fallahi-Sichani M, Sorger PK. Highly multiplexed imaging of single cells using a high-throughput cyclic immunofluorescence method. Nat Commun. 2015;6:1–7.
78. Lin J-R. Multiplexed single-cell imaging: past, present, and future. Assay Drug Dev Technol. 2016;15(1):8–10.
79. Todorovic V. A tissue-to-organelle view of cellular proteins. *Nat Methods*. 2018;15(10):760.
80. Bartman CR, et al. Transcriptional burst initiation and polymerase pause release are key control points of transcriptional regulation. *Mol Cell*. 2019;73(3):519–532.e4.
81. Rouhanifard SH, et al. ClampFISH detects individual nucleic acid molecules using click chemistry–based amplification. Nat Biotechnol. Nov. 2018;37:84.
82. Bridger JM, Morris K. Fluorescence in situ Hybridization (FISH), vol. 659. Totowa, NJ: Humana Press; 2010.
83. Cai L. Turning single cells into microarrays by super-resolution barcoding. Brief Funct Genomics. 2013;12(2):75–80.
84.•• Eng C-HL et al. Transcriptome-scale super-resolved imaging in tissues by RNA seqFISH+. Nature. 2019;568(7751):235–239. **This study scales up super-resoution barcoding to transcriptome level.**
85. Gratton E. Fluorescence lifetime imaging for the two-photon microscope: time-domain and frequency-domain methods. *J Biomed Opt*. 2003;8(3):381.
86. Funane T, et al. Selective plane illumination microscopy (SPIM) with time-domain fluorescence lifetime imaging microscopy (FLIM) for volumetric measurement of cleared mouse brain samples. *Rev Sci Instrum*. 2018;89(5):53705.
87. Digman MA, Caiolfa VR, Zamai M, Gratton E. The phasor approach to fluorescence lifetime imaging analysis. Biophys J. Jan. 2008;94(2):L14–6.
88. Cole MJ, Siegel J, Webb SED, Jones R, Dowling K, Dayel MJ, et al. Time-domain whole-field fluorescence lifetime imaging with optical sectioning. J Microsc. Sep. 2001;203(3):246–57.
89. Redford GI, Clegg RM. Polar plot representation for frequency-domain analysis of fluorescence lifetimes. *J Fluoresc*. 2005;15(5):805.
90. Martin ME, Wabuyele MB, Chen K, Kasili P, Panjehpour M, Phan M, et al. Development of an advanced hyperspectral imaging (HSI) system with applications for cancer detection. Ann Biomed Eng. Jun. 2006;34(6):1061–8.
91. Akbari H, et al. Hyperspectral imaging and quantitative analysis for prostate cancer detection. J Biomed Opt. Jul. 2012;17(7):1–11.
92. Cohen S, Valm AM, Lippincott-Schwartz J. Multispectral live-cell imaging. *Curr Protoc Cell Biol*. Jun. 2018;79(1):e46.
93.• Neher R, Neher E. Optimizing imaging parameters for the separation of multiple labels in a fluorescence image. *J Microsc*. 2004;213(1):46–62 **This paper shows how the figure of merit can be applied to a given imaging protocol to indicate how well it performs for a set of fluorophores.**
94. Pareja F, et al. Loss-of-function mutations in ATP6AP1 and ATP6AP2 in granular cell tumors. *Nat Commun*. 2018;9(1):3533.
95. Bendall SC, Simonds EF, Qiu P, Amir EAD, Krutzik PO, Finck R, et al. Single-cell mass cytometry of differential immune and drug responses across a human hematopoietic continuum. Science (80-). 2011;332(6030):687–96.
96. Carvajal-Hausdorf DE et al. Multiplexed (18-Plex) Measurement of Signaling Targets and Cytotoxic T Cells in Trastuzumab-Treated Patients using Imaging Mass Cytometry. Clin Cancer Res. 2019; 25(10):3054–3062.
97. Spitzer MH, Nolan GP. Mass cytometry: single cells, many features. Cell. 2016;165(4):780–91.
98. El-ad DA, et al. viSNE enables visualization of high dimensional single-cell data and reveals phenotypic heterogeneity of leukemia. Nat Biotechnol. Jun. 2013;31(6):545–52.
99. Schapiro D et al. histoCAT: analysis of cell phenotypes and interactions in multiplex image cytometry data. Nat Methods. 2017;14(9):873–876.
100. Schapiro D, Jackson HW, Raghuraman S, Fischer JR, Zanotelli VRT, Schulz D, et al. histoCAT: analysis of cell phenotypes and interactions in multiplex image cytometry data. Nat Methods. Sep. 2017;14(9):873–6.
101. van der Maaten L, Hinton G. Visualizing data using t-SNE Laurens. *J Mach Learn Res*. 2008;4:2579–605.
102. Allan C, Burel JM, Moore J, Blackburn C, Linkert M, Loynton S, et al. OMERO: flexible, model-driven data management for experimental biology. Nat Methods. Feb. 2012;9(3):245–53.